Semiconductors, 2025, Vol. 59, No. 1

Influence of emitter region doping level on the turn-on dynamics of low-voltage GaAs dynistors

© K.S. Zhidyaev, A.B. Chigineva, N.V. Baidus, I.V. Samartsev, A.V. Kudrin

Lobachevsky State University,
603022 Nizhny Novgorod, Russia

E-mail: zhidyaev@nifti.unn.ru

Received March 26, 2025
Revised April 16, 2025
Accepted April 17, 2025

A GaAs dynistors with mesa-strip has been fabricated and experimentally studied. It is shown that increasing the doping level of *n*- and *p*-emitters leads to a decrease in the turn-on time of GaAs dynistors and to an increase in their operation efficiency when generating nanosecond current pulses, namely to an increase in the amplitude and rate of rise of current and to a decrease in the rise time of the front.

Keywords: Thyristor, dynistor, gallium arsenide, turn-on dynamics, current pulse.

DOI: 10.61011/SC.2025.01.61075.7741

1. Introduction

Generation of nanosecond and subnanosecond current pulses with an amplitude of at least ~ 40 A and repetition rate of $20-200$ kHz for a low impedance load is currently an important task [1]. Such pulses are used, for example, for semiconductor laser pumping in laser range finding systems [2]. Short current pulse generation requires creation of fast current switches.

Various fast current switch versions are proposed in the literature. Many studies address the development and investigation of high-voltage silicon-based and gallium arsenide-based switches (transistors, thyristors, *S*-diodes) [1,3–5]. It is noted that an increase in the generation frequency ($\sim 10-100$ kHz) is followed by a sharp decrease in the pulse amplitude due to heating of the current switch structure [1].

Note that high-voltage switches appear to be ineffective, when load has a low resistance. Therefore significant research efforts were focused on the development of various low-voltage current switches operating at < 60 V. In [6], a pulse generator based on a GaN field-effect transistor was successfully implemented and current pulses with an amplitude of 1.1 kA, duration of 8 ns at a repetition rate of 10 kHz were generated. However, a decrease in the pulse duration to 580 ps caused a decrease in pulse amplitude to 30 A [7]. In addition, for effective functioning of GaN field-effect transistors, stringent requirements are established for quick response of the control circuit leading to an increase in its cost and weight-and-dimensional characteristics. To create compact short optical pulse sources, integration of thyristor structures an laser diodes appeared to be a promising technique. A low-voltage thyristor based on GaAs and GaAs solid solutions was an alternative option [8]. An array of such thyristors consisting of 6 elements generated current pulses with an amplitude of 60 A, duration of 6.4 ns and repetition rate of 1 MHz at 27 V for pumping a laser diode bar [9].

Several studies showed that the parameters of epitaxial layers included in the configuration of GaAs thyristor switches affected current pulse generation duration and amplitude [8,10,11]. Main focus in these studies was made on the epitaxial layers of base regions. However, to generate high-amplitude short current pulses, optimum parameters shall be also chosen for the emitter region layers of thyristor structures [12]. The study solves this problem and investigation of the influence of emitter region doping level on the GaAs dynistor activation behavior.

2. Test samples and experimental procedure

Two types of thyristor $p-n-p-n$-homostructures (Table 1) grown on n^+-GaAs (100) substrate by MOCVD. n^0- and p^0-type base regions ($2\,\mu$m each) were doped to $\sim 10^{16}\,\text{cm}^{-3}$. Structure differed in the parameters of emitter regions. In the first type structure, $0.5\,\mu$m and $0.1\,\mu$m *n*- and *p*-type emitters, respectively, were doped to $1 \cdot 10^{18}\,\text{cm}^{-3}$. In the second type structures, $0.3\,\mu$m emitters were formed and the concentration of dopant was reduced to $2 \cdot 10^{17}\,\text{cm}^{-3}$. The grown structures were used to make dynistors by etching stripe-geometry mesas with a depth of $0.5\,\mu$m and width of $360\,\mu$m. Ohmic contacts were made on the basis of AuGe. A stripe-geometry anode contact $300\,\mu$m in width was formed to the *p*-emitter, a solid cathode contact was formed to the n^+-GaAs substrate. Wafers with the fabricated structures were first split into bars with a mesastripe length of $1000\,\mu$m and then the bars were split into separate chips with a width of $800\,\mu$m (Figure 1).

The fabricated dynistor chips were mounted parallel to a 44 nF ceramic SMD capacitor. For switching current measurement, a 0.2 Ohm SMD resistor was additionally included in the circuit. Components were placed on a single board as close as possible to each other to reduce

Table 1. Description of the GaAs $p-n-p-n$ structures under study

Region	Type 1		Type 2	
	Thickness, μm	Doping, cm^{-3}	Thickness, μm	Doping, cm^{-3}
n-emitter	0.5	$1 \cdot 10^{18}$	0.3	$2 \cdot 10^{17}$
p^0-base	2.0	10^{16}	2.0	10^{16}
n^0-base	2.0	10^{16}	2.0	10^{16}
p-emitter	0.1	$1 \cdot 10^{18}$	0.3	$2 \cdot 10^{17}$

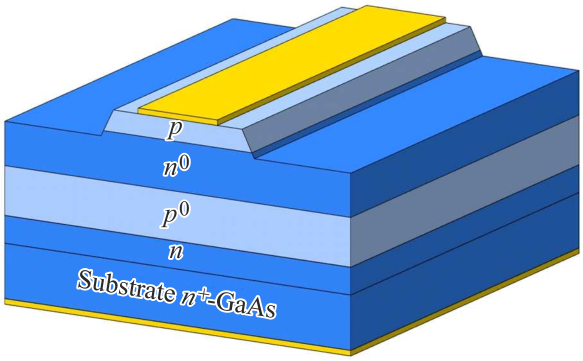

Figure 1. Schematic image of the chip of dynistors under study.

spurious effects. Dynistor turn-on was performed due to capacitor charging to switching voltage. Turn-on behavior was investigated with the fabricated switches operated in periodic mode at 300 Hz. Oscillograms of capacitor voltage $U_C(t)$ and resistor voltage $U_R(t)$ were recorded, from which time dependences of dynistor anode voltage $U_A(t) = U_C(t) - U_R(t)$ were derived. The study used an oscilloscope with passive probes with a 500 MHz band each.

3. Results and discussion

Static $I-U$characteristics of the dynistors under study measured in the current source mode were S-shaped (Figure 2). Samples were switched from off-state to on-state at $U_{BO} = 30$ V and $\sim 50\,\mu$A. In on-state at 4.5 mA, residual voltage of the both types of samples was 1 V, i. e. 3.3% of the breakover voltage.

Figure 3, a shows the curves of time vs. anode voltage of two types of dynistors during switching to the on-state. These curves were used to determine the rate of dynistor switching into the on-state as the time of anode voltage drop from 90% to 10% of the maximum voltage [13]. Type 1 structure was found to switch to the open state faster that type 2 structure (14 ns and 21 ns, respectively). The rate of switching into the on-state defines the switching current pulse shape (Figure 3, b). Dynamic parameters of current pulses generated using the dynistors under study are shown in Figure 2. It is shown that type 1 dynistors with higher doping level of emitter regions demonstrate more effective operation compared with type 2 dynistors. For type 1 dynistors, nanosecond current pulses with higher amplitude, shorter duration and pulse rise time were generated. Current rise rate (from 10% to 90% of the maximum current) for type 1 structure is twice as high than that for type 2 structure (13.7 A/ns and 6.1 A/ns, respectively). The last parameter is essential for generation of sharp-edge short current pulses. However, note that the current rise rate will depend heavily on the type of switch load.

Thyristors turn-on by means of accumulation of excess carriers (EC) in base regions. EC are necessary to compensate the bulk charge formed by p-type and n-type impurity ions of the collector (central) $p-n$-junction. It is known that two main mechanisms of excess carriers accumulation in bases may be implemented in dynistors. The first mechanism implies generation of electron-hole pairs by means of collision ionization in the electric field of reverse-biased collector $p-n$-junction formed by p- and n-type base regions. The second mechanism implies hole injection from the p-emitter into the n-base, hole diffusion into the electric field region of the collector $p-n$-junction and drift into the p-base. Electron diffusion and drift from the n-emitter into the n-base through the p-type base region take place in the same way. When two above-

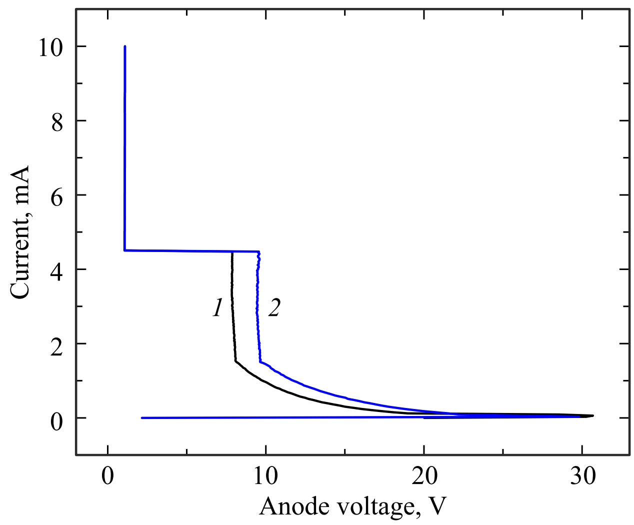

Figure 2. I–U characteristics of the dynistors under study: *1* — type 1, *2* — type 2.

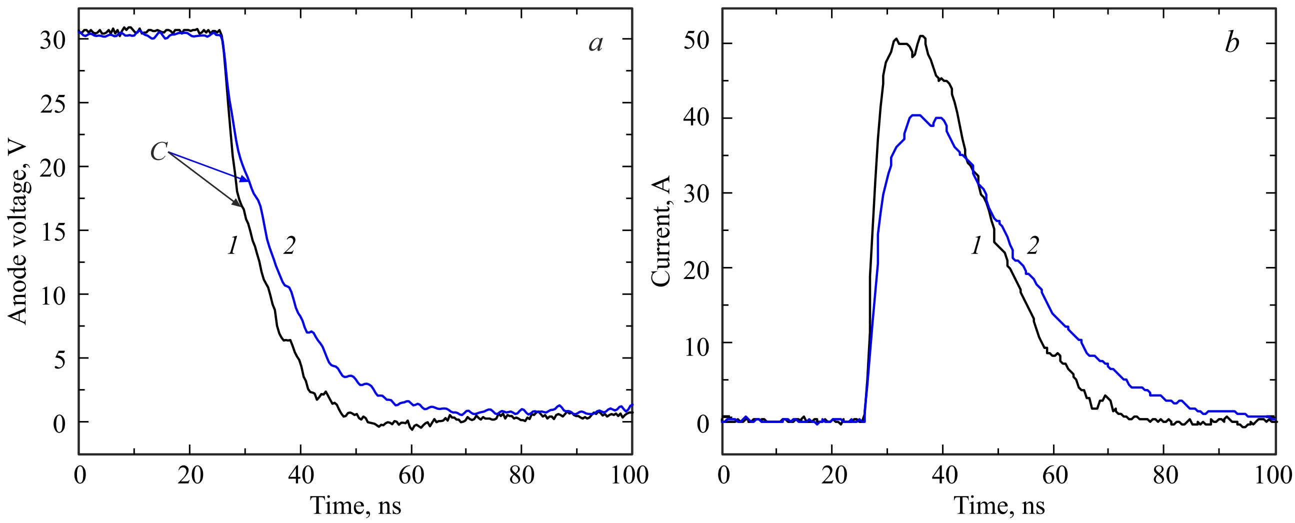

Figure 3. Time dependences of anode voltage (a) and current (b) of dynistors with $U_{BO} = 30$ V: *1* — type 1, *2* — type 2.

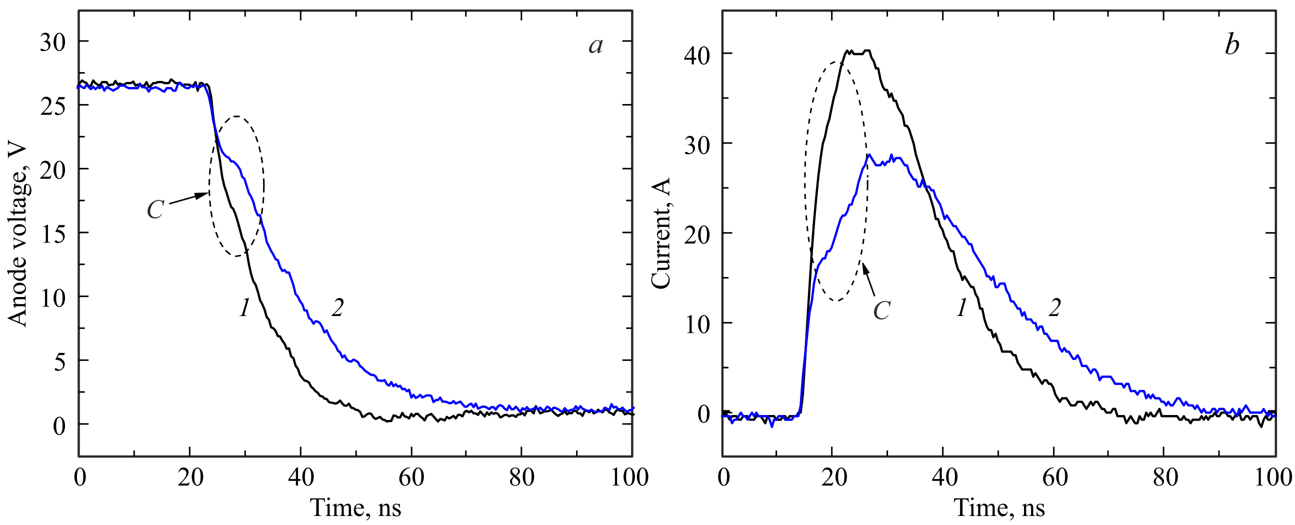

Figure 4. Time dependences of anode voltage (a) and current (b) of dynistors with $U_{BO} = 26$ V: *1* — type 1, *2* — type 2.

Table 2. Dynamic parameters of voltage and current measured for GaAs dynistors

Dynamic parameters	Dynistors with $U_{BO} = 30$ V		Dynistors with $U_{BO} = 26$ V	
	type 1	type 2	type 1	type 2
Voltage fall time, ns	14	21	16	29
Current pulse amplitude, A	51	41	40	29
Pulse duration, ns	21	26	23	34
Pulse rise time, ns	3	5	6	10
Current rise time, A/ns	13.7	6.1	5.5	2.3

mentioned mechanisms are present simultaneously, turn-on behavior will be first of all determined by a faster collision ionization process [11].

Review of the oscillograms (Figure 3) shows that at the initial turn-on stage (to ~ 1 ns from the start of current rise/voltage drop) anode voltage and current behavior is the same for two types of dynistors, but then turn-on of type 2 structure is decelerated a little with respect to type 1 structure. This may be associated with the fact that, at the initial turn-on stage, excess carriers accumulation mechanism is implemented in base regions of two types of dynistors due to the collision ionization. However, as the concentration of EC increases in the n- and p-bases, partial compensation of the bulk charge of ionized impurity takes place leading to electric field redistribution, i. e. to the reduction of maximum intensity and gradient [11]. Such electric field redistribution will induce the reduction of collision ionization rate and, consequently, to deceleration of dynistor turn-on. A small knee (Figure 3, a, point C) and decrease in the voltage fall rate are observed on the anode voltage oscillogram at this time. Contribution of the drift-diffusion mechanism of excess carriers accumulation in base regions will later have a greater influence on the turn-on behavior that at the initial stage. Efficiency of this mechanism will be defined by the emitter current transmission coefficient that depend on the injection coefficients that in turn depend on the ratio of emitter doping levels to bases [14]. Type 1 dynistors, have a doping level of emitter regions 5 times as high as that of type 2 dynistors with the same doping level of base regions. Therefore, the emitter current transmission coefficient in type 1 structure is higher and, consequently, the activation rate is higher at the time of collision ionization intensity reduction.

Study of the turn-on behavior of dynistors with similar designs having a switching voltage of $U_{BO} = 26$ V showed that (Figure 4) type 1 structure switched into the open state almost 2 times faster than type 2 structure (16 ns and 29 ns, respectively). Dynamic parameters of current pulses generated using such dynistors are shown in Table 2. It can be seen that, for both types of dynistors, as the breakover voltage decreases (from 30 V to 26 V), turn-on deceleration and, consequently, degradation of dynamic parameters of current pulses are observed. This is associated with the decrease in the collision ionization rate in base regions due to a decrease in maximum electric field intensity. Note that oscillograms of anode voltage and current of samples with $U_{BO} = 26$ V show more pronounced regions with deceleration of voltage fall and current rise behavior (Figure 4, regions C) than for samples with $U_{BO} = 30$ V (Figure 3). This is explained by the fact that the turn-on deceleration effect associated with a decrease in the collision ionization rate due to electric field redistribution in base regions will be more pronounced at lower switching voltages [11].

4. Conclusion

Thus, this study investigated the influence of the doping level of the n- and p-emitters on the turn-on behavior of low-voltage GaAs dynistors with stripe-geometry mesas. It is shown that for dynistors with a breakover voltage of 30 V, fivefold increase in the doping level of emitter regions leads to a decrease in turn-on time to the on-state by 30% (from 21 ns to 14 ns). The following parameters of generated nanosecond current pulses vary: amplitude increases from 41 A to 51 A, pulse rise time decreases from 5 ns to 3 ns and, consequently, the current rise rate increases more than twice from 6.1 A/ns to 13.7 A/ns.

Funding

The study was financially supported by the Ministry of Education and Science of the Russian Federation within the scope of the State Assignment (project FSWR-2023-0037).

Conflict of interest

The authors declare that they have no conflict of interest.

References

[1] S. Vainshtein, I. Prudaev, G. Duan, T. Rahkonen. Solid State Commun., **365** (7), 115111 (2023).
[2] J. Glaser. IEEE Power Electron. Mag., **4** (1), 25 (2017).
[3] S. Vainshtein, G. Duan, G.T. Rahkonen, Z. Taylor, V. Zemlyakov, V. Egorkin, O. Smolyanskaya, T. Skotnicki, W. Knap. Results Phys., **19**, 103509 (2020).
[4] S.N. Vainshtein, A. Kilpela, J. Kostamovaara, R. Myllyla, S. Starobinets, Ju. Zhilyaev. IEEE Trans. Electron Dev., **41** (8), 1444 (1994).
[5] S.N. Vainshtein, V.S. Yuferev, J.T. Kostamovaara, M.M. Kulagina, H.T. Moilanen. IEEE Trans. Electron Dev., **57** (4), 733 (2010).
[6] N. Ammouri, H. Christopher, J. Fricke, A. Ginolas, A. Liero, A. Maaßdorf, H. Wenzel, A. Knigge. Electron. Lett., **59** (1), e12680 (2023).
[7] A. Liero, A. Klehr, T. Hoffmann, T. Prziwarka, W. Heinrich. *Proc. 46th Eur. Microw. Conf. (EuMC)* (London, UK, Oct. 2016) p. 1389.
[8] S.O. Slipchenko, A.A. Podoskin, I.V. Shushkanov, V.A. Kryuchkov, A.E. Rizaev, M.I. Kondratov, A.E. Grishin, N.A. Pihtin, T.A. Bagaev, V.N. Svetogorov, M.A. Ladugin, A.A. Marmalyuk, V.A. Simakov. Pis'ma ZhTF, **50** (4), 43 (2024). (in Russian).
[9] S.O. Slipchenko, A.A. Podoskin, V.V. Zolotarev, L.S. Vavilova, A.Yu. Leshko, M.G. Rastegaeva, I.V. Miroshnikov, I.S. Shashkin, N.A. Pikhtin, T.A. Bagaev, M.A. Ladugin, A.A. Padalitsa, A.A. Marmalyuk, V.A. Simakov. Phys. Inst., **50** (5), S527 (2023).
[10] S.O. Slipchenko, A.A. Podoskin, I.V. Shushkanov, V.A. Kryuchkov, A.E. Rizaev, M.I. Kondratov, A.E. Grishin, N.A. Pihtin, T.A. Bagaev, V.N. Svetogorov, M.A. Ladugin, A.A. Marmalyuk, V.A. Simakov. FTP, **57** (8), 678 (2023). (in Russian).
[11] O.S. Soboleva. Cand. dis. (SPb., FTI im A.F.Ioffe, 2022). (in Russian).
[12] A. Blicher. *Thyristor physics* (N.Y.–Heidelberg–Berlin, Springer Verlag, 1976).
[13] S.O. Slipchenko, O.S. Soboleva, A.A. Podoskin, Yu.K. Kirichenko, T.A. bagaev, I.V. Yarotskaya, N.A.P ikhtin. FTP, **57** (4), 295 (2023). (in Russian).
[14] V.A.Gurtov. *Tverdotelnaya electronika:* Ucheb.posobie, 2e izd., pererab.i dop. (M., 2005). (in Russian).

Translated by E.Ilinskaya